PCCP

Accepted Manuscript

ROYAL SOCIETY OF CHEMISTRY

www.rsc.org/pccp

Physical Chemistry Chemical Physics

ARTICLE

Adsorption of Ozone and Plasmonic Properties of Gold Hydrosol: Effect of Nanoparticles Size

Received 00th January 20xx,
Accepted 00th January 20xx

DOI: 10.1039/x0xx00000x

www.rsc.org/

Boris G. Ershov*, Evgeny V. Abkhalimov, Vyacheslav I. Roldughin, Viktor M. Rudoy, Olga V. Dement'eva, Roman D. Solovov

The impact of size of gold nanoparticles on the magnitude of bathochromic shift of their plasmon resonance peak upon ozone adsorption is revealed and analyzed. Namely, the plasmon band position of 7, 10, 14 and 32 nm nanoparticles shifts toward longer wavelengths by 51, 35, 23 and 9 nm respectively, *i.e.* the smaller the nanoparticles, the greater the shift of the band. Thus, the sensor efficiency of gold hydrosol increases with a decrease in the nanoparticle size. The shift of the Fermi level is a linear function of the inverse radius of nanoparticles. The observed alterations in the gold nanoparticles plasmonic properties and the Fermi level position are explained by a decrease in electron density of nanoparticles caused by the electrons' partial binding by adsorbed O_3 molecules. The insignificance of oxygen and nitrous oxide effect on plasmonic properties of gold hydrosol is observed.

Introduction

The creation of bio- and chemosensory systems based on the change in the optical characteristics of gold hydrosol upon the analyte/nanoparticles interaction is one of the most promising fields of modern nanotechnology. Raman and localized surface plasmon resonance (LSPR) spectroscopies are widely used for this purpose. High sensitivity of gold nanoparticle LSPR to the composition of the environment allows one to use them to create effective sensors for selective detection of various substances (*e.g.* heavy metal ions,[1,2] gases[3-5] and organic compounds[2,6]), as well as to solve a wide range of analytical problems in biochemistry and biomedicine.[2,7-12] In particular, it was revealed[3] that the reversible bathochromic shift of 25 nm gold nanoparticles' plasmon band takes place at the saturation of the colloidal solution with ozone-oxygen mixture. Later, it was proposed[4] to use this effect for gaseous ozone detection with a sensitivity of ~ 10 ppb.

It is well known that the optical properties of Au and Ag hydrosols essentially depend on particle size and shape.[13,14] Thus, the size of gold nanospheres can be accurately enough predicted even by hydrosol color. A response to an external action – in particular, to the presence of an analyte in a solution – obviously depends on the nanoparticle size as well. Our previous studies[15,16] shown that the bathochromic shift of LSPR of gold nanoparticles with average diameter of 7 nm upon hydrosol saturation with ozone was more pronounced than one registered for the larger particles.[3,4] This indicates the possible presence of a size effect in the interaction of ozone with colloidal gold.

Herein, we report new data evidencing the size effect in plasmon absorption of gold hydrosol nanoparticles upon ozone adsorption. We also give a theoretical background for the observed phenomenon. In our opinion, this "size effect" paves the way for the optimization of gold hydrosol-based sensor's characteristics.

Experimental

Preparation of Au nanoparticles

Gold hydrosols with particle average diameter from 7 to 32 nm stabilized by citrate anions were studied. Hydrosols were synthesized using tetrachloroauric acid trihydrate as precursor and trisodium citrate dihydrate or sodium borohydride as reducing agent;[15-17] all of the reagents were of ACS Reagent Grade and purchased from Aldrich. Distilled water was additionally deionized with an Arium setup (Sartorius) before being used for solution preparation.

Characterization

The absorption spectra of gold colloidal solutions were measured at fixed time intervals (up to several days) using a Cary 100 Scan UV-Visible spectrophotometer (Varian Inc.) equipped with a thermostated cuvette compartment at 20 °C (wavelength range 190-900 nm, bandwidth 2 nm, integration time 0.1 s, data interval 1 nm, scan speed 600 nm/min^{-1}).

A.N. Frumkin Institute of Physical Chemistry and Electrochemistry, Russian Academy of Science, Leninsky pr. 31-4, Moscow, 119071, Russia
E-mail: ershov@ipc.rssi.ru, abkhalimov@ipc.rssi.ru

Gold nanoparticle sizes as well as values of their ζ-potential were determined before and after the ozonation of the colloidal solution by dynamic light scattering technique. The measurements were performed with a Zetasizer Nano ZS instrument (Malvern) at a wavelength of 633 nm using the Dispersion Technology Software for data collection and analysis. Prior to the onset of the measurements, the examined solution was thermostated at 20 °C.

The sizes and shapes of the gold nanoparticles were also analyzed in a Leo-912 AB Omega (Carl Zeiss) and JEM-2100 (JEOL) transmission electron microscope. For this purpose, a droplet of a colloidal solution was kept on a formvar-coated copper grid for 30 s and then removed with filter paper. The images were processed using Gwyddion software.[18] The histograms were computed using ImageJ (NIH) on a minimum of 100 randomly selected nanoparticles.

Ozonation

Ozone-oxygen mixture with O_3 concentration of 150 $mg \cdot L^{-1}$ was produced from pure oxygen in a special ozone generator. The experiments on ozone adsorption on Au nanoparticles were performed as follows. An aliquot of desired gold colloidal solution (5 mL) was placed into a special cell equipped with a quartz cuvette with a light path of 5.0 or 10.0 mm. The design of the cell made it possible to evacuate it and to isolate its internal volume from the environment. Then ozone was bubbled (with flow rate of 0.5 $mL \cdot s^{-1}$) through the colloidal solution for preset time periods (from 8 s to 60 min). After the optical spectrum was measured, ozone was removed from the colloidal solution with a vacuum pump for 20-30 s. After this, the residual ozone concentration in the solution did not exceed 10^{-6} mol L^{-1}.

Results and Discussion

Fig. 1 shows the variations in the absorption spectra of gold sol with average diameter of nanoparticles of 7 nm after its saturation with ozone-oxygen mixture and subsequent evacuation. It can be seen that the original LSPR band of the sol at 510 nm (curve 1) shifts to longer wavelengths upon ozonation, and after about 40 min reaches the "final" position at a wavelength of 561 nm (curve 2). The bathochromic shift of the plasmon band is accompanied by a noticeable decrease in the band intensity and its broadening (see inset on Fig. 1). After the ozone is removed by evacuation of the system, the position and shape of the LSPR band are gradually (in about 8 h) restored (Fig. 1) and then remain unchanged for several days. The colloidal gold concentration does not decrease during hydrosol saturation by ozone and its evacuation. This means that ozone does not oxidize the gold hydrosol in contrast with a silver hydrosol.[20] The bathochromic shift of the plasmon band of gold nanoparticles during the sol ozonation is, obviously, caused by O_3 adsorption on their surfaces and "binding" of the nanoparticle conduction electrons. The restoration of the band results from desorption and/or decomposition of ozone. Repeating the ozone adsorption/desorption procedure is accompanied by reversible changes in the LSPR band position. The processes of ozone adsorption and desorption are relatively slow; and system equilibrium is determined by the concentration of ozone in the solution. Thus, bubbling the ozone through the colloidal solution for 2–5 min leads to the plasmon band bathochromic shift (approximately to 550 nm) evolving over time (within 20 to 30 min). However, when ozone is passed continuously for about 40 min, the shift of plasmon band up to 561 nm takes place. In this case, the concentration of dissolved ozone calculated by its absorption at λ_{max} = 258 nm (curve 2, Fig. 1) and molar extinction coefficient ε = 2900 mol^{-1} cm^{-1} is equal to approximately 7×10^{-4} $mol \cdot L^{-1}$.[19] It can be assumed that the increase in O_3 concentration will lead to an even more pronounced shift of the plasmon band.

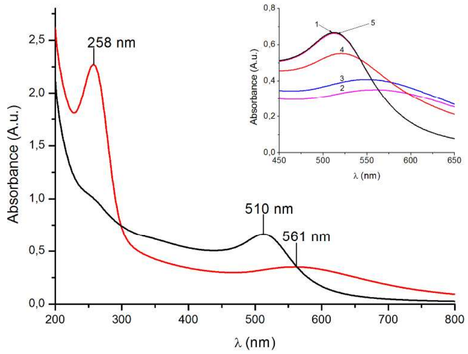

Fig. 1. Absorption spectra of gold hydrosol with average particles' diameter of 7 nm: (1) initial hydrosol, (2) after 40 min bubbling of ozone-oxygen mixture, (3–5) after evacuation of the system for 1, 2, and 8 h, respectively. The spectral region of 450–650 nm is shown in the inset.

The effect of LSPR reversible bathochromic shift upon ozone adsorption/desorption is also revealed for gold nanoparticles with diameters of more than 7 nm.[15,16] In this case, however, the larger the nanoparticles, the smaller the plasmon band shift, caused by ozone adsorption (see Fig. 2). Thus, the "initial" λ_{max} values corresponding to the LSPR of gold nanoparticles with average diameters of 10, 14 and 32 nm are equal to 514, 517 and 526 nm respectively; after ozone adsorption the λ_{max} values shift to long-wave region for 35, 23 and 9 nm (see Fig. 2). The plasmon band recovery time after desorption of ozone is decreased substantially (from 3 h to 10 min) with an increase in particle size from 10 to 32 nm. Let us recall that the bathochromic shift of LSPR of 7 nm gold nanoparticles is equal to 51 nm; the recovery time of plasmon band for such particles is about 8 h. Thus, the gold nanoparticles' size substantially affects both the ozone adsorption/desorption kinetics and the LSPR shift values. The smaller the metal nanoparticles, the greater the shift of the LSPR band. Moreover, decreasing in gold nanoparticles' size leads to the increase of ozone desorption time. Presumably, this effect is caused by the reduction of the binding energy of ozone molecules with gold surfaces with an increase in the nanoparticle size.

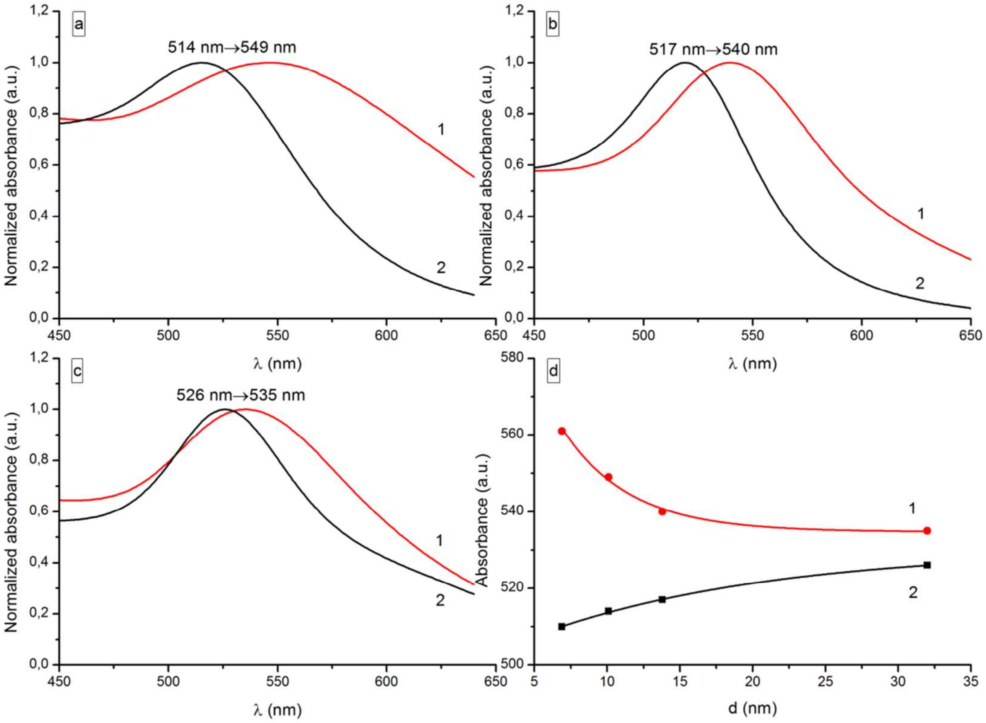

Fig. 2. Absorption spectra of gold hydrosols with average particles' diameter of 10 (a), 14 (b), and 32 nm (c): before (1) and after ozonation (2). Shift of absorption band of gold hydrosol before and after ozonation from the size of particles (d).

It should be pointed out, if the ozonation time doesn't exceed 40 min, the nanoparticle size distribution doesn't change substantially (see, for example, Fig. 3). The ζ-potential values of the sol nanoparticles are -40 to -50 mV, *i.e.* the citrate ions adsorbed onto gold nanoparticles provide their stability against coagulation. When ozonation is prolonged, the sols lose their stability due to the complete oxidation of the citrate ions present therein.[15,16]

It is interesting to compare the influence of other gases on the plasmonic properties of the gold hydrosol. Effect of O_2 and N_2O is found for only small particles (≤10 nm). For example, 3 and ~ 1 nm shift of absorption band, respectively, for O_2 and N_2O is observed for the particles with diameter of 7 nm (Fig. 4). The absorption band immediately comes back to the initial state after degassing. That is due to essential weaker bond strength of oxygen and nitrous oxide with a gold surface. Practically, air does not affect optical absorption of hydrosol.

It is well known that the plasmon absorption of metal nanoparticles is caused by the excitation of collective oscillations of the free conduction electrons. The frequency of these collective oscillations (plasmons) is mainly determined by the effective electron density.[21] For this reason, the plasmon resonance frequency is sensitive to the redox properties of nanoparticles' environment.[22-26] If electrons transfer from an environment to nanoparticles (*i.e.* their effective density increases), the LSPR band shifts to the short-wave region. When the "drawing off" of the electrons from the nanoparticles takes place and their effective density decreases, the plasmon band shifts in the opposite direction.

Although the plasmon is a collective quantum excitation its resonance frequency can be calculated using classical approximation.[21] The optical properties of metal nanoparticles are well described by Mie–Drude theory;[27,28] according to this

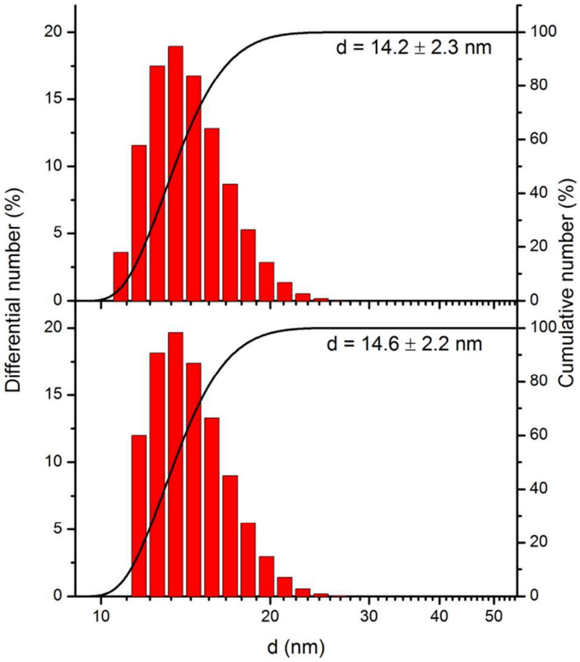

Fig. 3. Histograms of the particle size distribution of gold hydrosol with average particles diameter of 14 nm: before (top) and after ozonation (bottom).

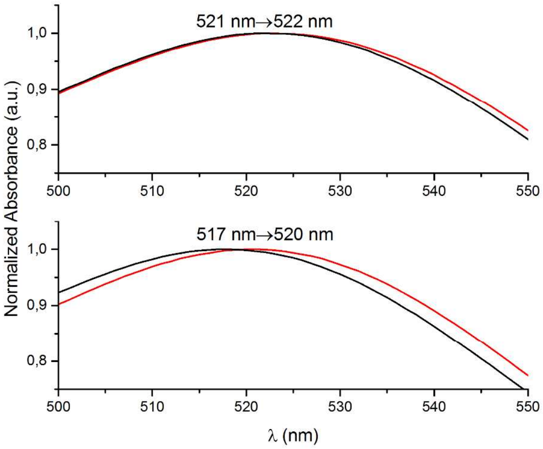

Fig. 4. Absorption spectra of gold hydrosol with average particles' diameter of 7 nm: before (black line) and after bubbling (red line) of N_2O (top) and O_2 (bottom).

theory, the LSPR band position is determined by the following equation:

$$\lambda_{\max}^2 = \frac{(2\pi c)^2 m(\varepsilon_0 + 2n)}{4\pi N_e e^2} \qquad (1)$$

where c is the speed of light; m and e are the electron effective mass and charge, respectively; ε_0 is the metal permittivity; n is the refractive index of surrounding medium; and N_e is the concentration of conduction electrons in a metal. It can be seen that an increase in N_e should lead to a "blue" shift of the plasmon absorption band and a decrease in N_e to a “red” shift. According to Eq. (1), the LSPR band position depends on the effective electron density in a nanoparticle, but not on its size. At the same time, the dependence of the LSPR band position on the nanoparticle size is well established experimentally.[27,28] This dependence is relevant to the secondary effects, such as variations in the frequency of collisions between electrons and the nanoparticle surface, quantization of energy levels, and variations in the effective electron density in nanoparticles. The last effect is caused by the electrons' ability to “go out” of the nanoparticle (due to quantum effects) for some distance.

The Eq. (1) permits us to connect the LSPR position and the concentration of conduction electrons in a metal particle before and after adsorption of analyte onto its surface:

$$\frac{\lambda_i^2}{\lambda_f^2} = \frac{N_{e,f}}{N_{e,i}} \qquad (2)$$

where the subscripts “i” and “f” refer to the system’s initial and final states, respectively. It should be pointed out that all other system parameters are excluded from the relation (2), so there is no need to determine m, ε_0 and n magnitudes. These parameters are only necessary to determine the absolute values of λ_i и λ_f. Thus, the relation (2) makes it possible to judge the change in the relative electron concentration in a metal by the shift of an LSPR band upon an external action on nanoparticles.

Fig. 5 shows the dependence of $N_{e,f}/N_{e,i}$ on λ_{max} for gold nanoparticles in the wavelength range of 510–570 nm. As follows from comparison of the experimental data obtained for the effect of ozone on the position of the LSPR band of 7 nm gold nanoparticles with calculation results, an adsorption of ozone molecules leads to the shift of the plasmon band from 510 to 561 nm and to the reducing the electron concentration in the metal by 17.1 %. Thus, the chemisorption shifts the electron density of the metal toward the adsorbate; this is accompanied by a decrease in the Fermi energy (Fig. 6). The color of gold hydrosol is also changed.

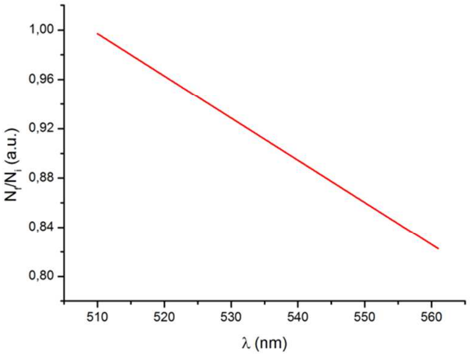

Fig. 5. Dependence of relative concentration of electrons in a gold nanoparticle vs. the position of the LSPR band.

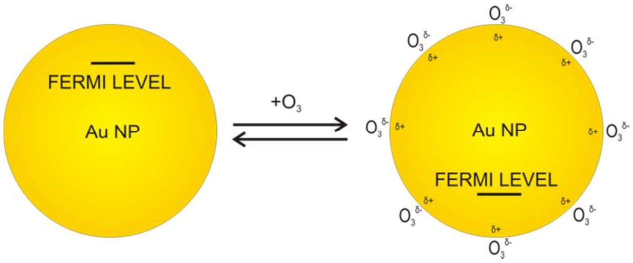

Fig. 6. Schematic representation of ozone adsorption–desorption on a gold nanoparticle and the concomitant shift of the Fermi level.

The weak influence of O_2 and N_2O on plasmonic properties of gold hydrosol (LSPR shift is 3 nm and ~1 nm, respectively) has been noted. Calculations (equation 2) show their adsorption on gold would reduce electron density in the metal, respectively, only by ~0.7 % and ~0.3 %. The efficiency of adsorption substantially depends on the electron affinity of adsorbate. Thus, electron affinity decreases significantly in order O_3, O_2 and N_2O (2.1, 0.45 and 0.03 eV, respectively)[31] that correlates with influence of these gases on plasmonic properties of gold hydrosol. It was proposed[3,4] to use this effect for gaseous ozone detection with a sensitivity of ~ 10 ppb. We foresee same effect with other gases which have greater electron affinity than N_2O and O_2. For example, the electron affinity of SO_2, NO_2 and Cl_2 are 1.11, 2.27, 2.38 eV, respectively[31]. High sensitivity of gold nanoparticle LSPR to the composition of the environment allows one to use them to create effective sensors for selective detection of O_3 and also mentioned gases.

Let us estimate the dependence of the shift of Fermi level upon ozone adsorption on the nanoparticle size. We assume that ozone molecules "draw off" electrons from a metal particle in such a way that the radius of the region of electron spatial distribution enlarges by a value of r_0 to compare with the particle radius R. At the same time, we suppose that $r_0 << R$ and this value doesn't depend on the particle size. The parameter r_0 can be treated as Thomas-Fermi screening length $r_0 \approx r_{\mathrm{TF}}$, where $r_{\mathrm{TF}} = [\hbar^2\pi^{1/3}/4me^2(3N_e)^{1/3}]^{1/2}$.[21] For metals the value of r_{TF} is approximately equal to 0.5–1 Å.

In the considered approach adsorption of ozone is treated as an effect of symmetrical external electric field. We understand that in some cases this may be a reasonable assumption for relatively large spherical nanoparticles covered by a rather uniform adsorbate layer. The justification for the use of this approach in our case is the following fact. The plasmons are collective motion of the electrons. Therefore, at excitation the electron density can be considered spread over the volume the nanoparticles. This allows using the scheme proposed above, even in the presence on the particle surface of only a small number of the adsorbed molecules. The discrete structure of the adsorbate will manifest itself when considering the more subtle effects.

It is quite obvious that the number of electrons in the nanoparticle upon ozone adsorption remains unchanged. Only the spatial region of electron distribution changes (increases). Under these assumptions, the electron density of nanoparticles is reduced upon ozone adsorption according to the change of the volume available for electrons:

$$N_{\mathrm{e,f}} = N_{\mathrm{e,i}}\frac{R^3}{(R+r_0)^3} \approx N_{\mathrm{e,i}}(1-\frac{3r_0}{R}) \qquad (3)$$

When deriving this equation the smallness of r_0 compared to the R was taken into account.

To determine the Fermi energy as a function of the electron density N_e the classical equation[29] were used:

$$E_{\mathrm{F}} = \frac{\hbar^2(3\pi^2N_e)^{2/3}}{2m_0} \qquad (4)$$

This equation shows that Fermi level decreases with a reduction in electron concentration. Upon ozone adsorption, this effect manifests itself as a shift of the LSPR band to the red spectral region. The shift of the Fermi level (ΔE_F) is described by the following equation:

$$\Delta E_{\mathrm{F}} \approx \left(\frac{2}{3}\right)E_{\mathrm{F}}\frac{N_{\mathrm{e,i}}-N_{\mathrm{e,f}}}{N_{\mathrm{e,i}}} \approx \left(\frac{2}{3}\right)E_{\mathrm{F}}\frac{3r_0}{R} \approx \left(\frac{2}{3}\right)E_{\mathrm{F}}\left(1-\frac{\lambda_{\mathrm{i}}^2}{\lambda_{\mathrm{f}}^2}\right) \qquad (5)$$

Factor $\varphi=(N_{e,i}-N_{e,f})/N_{e,i}$ takes into consideration the relative reduction in the electron concentration in a metal. Note that, as mentioned above, the plasmon absorption and, respectively, the Fermi energy value are associated with the particle size. Thus, it would be more correct to use the $E_F(R)$ function instead the E_F in the Eq. (5). However, taking into account this size dependence leads to the "higher order" changes of ΔE_F, which are beyond the approximations used.

Table 1. The shifts in the position of the maximum of plasmon resonance and the Fermi level depending on gold nanoparticle diameter.

D, nm	$\lambda_i - \lambda_f$, nm	ΔE_F, eV
7.0	51	0.64
10.0	35	0.45
14.0	23	0.31
32.0	9	0.12

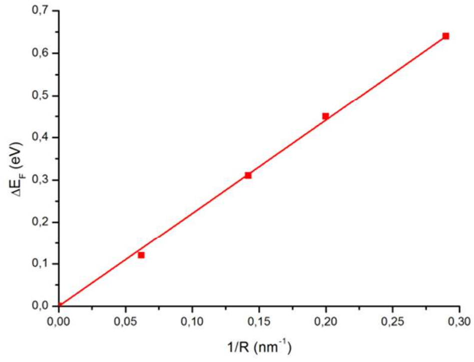

Fig. 7. Shift of the Fermi level in gold nanoparticles as calculated from the LSPR band shift vs. inverse particle radius.

For gold, Fermi energy E_F = 5.5 eV. Assume it is constant, and define the φ values by the shifts of the plasmon band for gold nanoparticles of different sizes. The ΔE_F values determined from the Eq. (5) are listed in the table 1. It can be seen that these values are in the range that corresponds to the experimental data obtained by, for example, measuring the work function for a metal surface in the presence of an adsorbate (1 eV approximately).[30]

For particles with sizes of 7–32 nm, the aforementioned cause of the shift in the position of the maximum plasmon resonance upon ozone adsorption seems to be quite reasonable. This is confirmed by the dependence of the shift in the Fermi energy on nanoparticle size depicted on Fig. 7, which is well approximated by a straight line in the ΔE_F–$1/R$ coordinates. In our view, the linearization of the dependence plotted from experimental data is a convincing argument for the mechanism, which is proposed for the shift in the plasmon band of nanoparticles upon ozone adsorption and for the reasonableness of the assumptions used in deriving the quantitative correlation between the change in the Fermi energy and the LSPR band position. It should also be mentioned that the revealed decrease in ΔE_F with the increase of the gold nanoparticles' size is well correlated with a decrease in ozone desorption time, which we pointed out earlier. Thus, the energy of chemisorption (the strength of the bond between the adsorbate and the metal surface) is reduced upon the transition from small gold nanoparticles to larger ones.

Conclusions

Thus, it may be stated that a shift in the plasmon resonance band of gold hydrosols upon ozone adsorption on their nanoparticles is, mainly, governed by a decrease in the effective electron density of particles. Moreover, the shift of the Fermi level is a linear function of the nanoparticle inverse radius. Hence, when using a gold hydrosol as a sensor for electrophilic or nucleophilic compounds which adsorption onto nanoparticles' surface will influence the LSPR position, the sensitivity of this sensor may be expected to increase with a decrease in the nanoparticle size. This conclusion is obviously also valid for solid-state sensors, which working elements are ensembles of gold nanoparticles formed on various substrates. Of course, the aforesaid remains valid for the plasmonic nanoparticles of other metals.

Acknowledgements

This work was supported by the Russian Foundation for Basic Research, project no. 15-03-02068-a.

Notes and references

1 A. Sugunan, C. Thanachayanont, J. Dutta, J.G. Hilborn, *Sci. Tech. Adv. Mater.*, 2005, **6**, 335-340.
2 K. Saha, S.S. Agasti, C. Kim, X. Li, V.M. Rotello, *Chem. Rev.*, 2012, **112**, 2739-2779.
3 S.D. Puckett, J.A. Heuser, J.D. Keith, W.U. Spendel, G.E. Pacey, *Talanta*, 2005, **66**, 1242-1246.
4 A.N. Pisarenko, W.U. Spendel, R.T. Taylor, J.D. Brown, J.A. Cox, G.E. Pacey, *Talanta*, 2009, **80**, 777-780.
5 D. Buso, M. Post, C. Cantalini, P. Mulvaney, A. Martucci, *Adv. Funct. Mater.*, 2008, **18**, 3843-3849.
6 K.-J. Chen, C.-J. Lu, *Talanta,* 2010, **81**, 1670-1675.
7 E. Hutter, J.H. Fendler, *Adv. Mater.*, 2004, **16**, 1685-1706.
8 N.L. Rosi, C.A. Mirkin, *Chem. Rev.*, 2005, **105**, 1547-1562.
9 M.E. Stewart, C.R. Anderton, L.B. Thompson, J. Maria, S.K. Gray, J.A. Rogers, R.G. Nuzzo, *Chem. Rev.*, 2008, **108**, 494-521.
10 N.G. Khlebtsov, L.A. Dykman, *J. Quant. Spectrosc. Radiat. Trans.*, 2010, **11**, 1-35.
11 K.M. Mayer, J.H. Hafner, *Chem. Rev.*, 2011, **111**, 3828-3857.
12 E. Petryayeva, U.J. Krull, *Anal. Chim. Acta*, 2011, **706**, 8-24.
13 K.L. Kelly, E. Coronado, L.L. Zhao, G.C. Schatz, *J. Phys. Chem. B*, 2003, **107**, 668-677.
14 V.A. Bogatyrev, L.A. Dykman, B.N. Khlebtsov, N.G. Khlebtsov, *Opt. Spectrosc.*, 2004, **96**, 128-135.
15 P.A. Morozov, B.G. Ershov, E.V. Abkhalimov, O.V. Dement'eva, T.B. Rumyantseva, V.M. Rudoy, V.I. Roldughin, *Coll. J.*, 2011, **73**, 668-675.
16 P.A. Morozov, B.G. Ershov, E.V. Abkhalimov, O.V. Dement'eva, M.A. Filippenko, V.M. Rudoy, V.I. Roldughin, *Coll. J.*, 2012, **74**, 502-509.
17 G. Frens, *Nature Phys. Sci.*, 1973, 241, 20-22.
18 D. Necas, P. Klapetek, *Cent. Eur. J. Phys.*, 2012, **10**, 181–188.
19 H. Bader, J. Holgne, *Ozone: Sci. Eng.* 1982, **4**, 169-176.
20 P.A. Morozov, E.V. Abkhalimov, A.E. Chalykh, S.A. Pisarev, and B.G. Ershov, *Coll. J.*, 2011, 73, 248–252.
21 D. Pines, *Elementary Excitations in Solids*, W.A. Benjamin Inc, New York, 1963.
22 P. Mulvaney, *Langmuir*, 1996, **12**, 788-800.
23 T. Ung, M. Giersig, D. Dunstan, P. Mulvaney, *Langmuir*, 1997, **13**, 1773-1782.
24 B.G. Ershov, A.V. Gordeev, *Mend. Commun.*, 2001. **11**, 147-148.
25 V.I. Roldughin, *Russ. Chem. Rev.*, 2000, **69**, 821-843.
26 P. Mulvaney, J. Pérez-Juste, M. Giersig, L.M. Liz-Marzán, C. Pecharromán, *Plasmonics*, 2006, **1**, 61-66.
27 C.F. Bohren, D.R. Huffman, *Absorption and Scattering of Light by Small Particles*, Willey, New York, 1983.
28 U. Kreibig, M. Vollmer, *Optical Properties of Metal Clusters*, Springer, Berlin, 1995.
29 L.D. Landau, E.M. Lifshitz, *Statistical Physics, Part 1*, Pergamon, New York, 1980.
30 M.W. Roberts, C.S. McKee, *Chemistry of the metal-gas interface*, Clarendon Press, Oxford, 1978.
31 *CRC Handbook of Chemistry and Physics*, Editor: D.R. Lide, CRC Press, Boca Raton, FL, 2005.